DIGITAL ATLAS OF RAINFALL DESIGN INTENSITIES IN SLOVAKIA

MILAN ONDERKA[1,2*], MAREK SOKÁČ[4], KATARÍNA MIKULOVÁ[1], JOZEF PECHO[1,3]

[1] *Slovak Hydrometeorological Institute, Jeséniova 17, Bratislava, Slovakia SK-83315*
[2] *Earth Science Institute, Slovak Academy of Sciences, Dúbravská cesta 9, Bratislava, Slovakia SK-84005*
[3] *Comenius University, Faculty of Mathematics, Physics and Informatics, Bratislava, Slovakia, SK-84248*
[4] *Institute of Hydrology, Slovak Academy of Sciences, Dúbravská cesta 9, Bratislava, Slovakia SK-84005*
[*] *Corresponding author's email: milan.onderka@savba.sk*

Relationships between rainfall intensities, duration and frequency, graphically displayed in the form of Intensity-Duration-Frequency (IDF) curves, are important for the design a variety of storm water management structures. The calculation of rainfall frequency estimates in Slovakia has been historically the responsibility of the national weather service (nowadays the Slovak Hydrometeorological Institute). The digital atlas (a multidimensional array) comprising 224 raster layers with rainfall intensities corresponding to return periods 2, 5, 10, 20, 30, 50 and 100 years, and rainfall durations lasting 5, 10, 15, 20, 30, 40, 50 and 60 minutes; 90 minutes, and 2, 3, 6, … up to 24 hours, is presented for the entire territory of Slovakia. Time series of 1-minute rainfall recorded by automatic and mechanical self-registering rain gauges (digitalized strips) were first checked for quality and aggregated to selected temporal scales. Annual maxima series were calculated for each location. Due to the relatively short time series of rainfall measurements (< 20 years), the parameters of the GEV distribution function were inferred by the Bayesian approach using the annual maxima series (AMS) method. The derived local estimates of rainfall frequencies were spatially interpolated in order to derive accurate estimates of rainfall frequencies for locations without in-situ rainfall measurements. From various geostatistical methods described in the literature that can be used for interpolating rainfall data from observations made at scattered locations into a regularized grid of points, we chose tri-variate Regularized Splines with Tension (v.vol.rst) implemented within the GRASS geographic information system. This method allowed us to incorporate altitude as a covariate. This enabled us to account for the influence of orography on rainfall intensities. The horizontal resolution of the resulting maps of gridded rainfall frequencies is 500 meters. The individual data arrays were stacked into a multidimensional cube from which we can abstract IDF curves specifying the requested return level for any location within the territory of Slovakia. Examples displaying the derived maps illustrate the spatial variability of rainfall intensities. A graphical interface will have to be created to facilitate the use of the presented work by the climatological service of the Slovak Hydrometeorological Institute.

Vzťahy medzi intenzitou dažďa, s jeho trvaním a frekvenciou výskytu, ktoré sú v grafickej podobe známe tiež ako IDF krivky (z angl. Intensity-Duration-Frequency), sú dôležitou pomôckou pre vodohospodársku prax. Výpočet návrhových hodnôt intenzít atmosférických zrážok na Slovensku je historicky úlohou klimatologickej služby Slovenského hydrometeorologického ústavu. Digitálny atlas (vo forme multidimenzionálneho dátového poľa) pozostávajúci z 224 dátových polí s intenzitami dažďa korešpondujúcimi s dobou opakovania T = 2, 5, 10, 20, 30, 50 a 100 rokov, pre dĺžky dažďových oddielov od 5, 10, 15, 20, 30, 40, 50 a 60 minút; 90 minút, a ďalej 2, 3, 6, … až po 24 hodín, je po prvýkrát prezentovaný pre celé územie Slovenska. Na jeho vytvorenie boli použité údaje z automatických zrážkomerov a digitalizovaných ombrografických pások s časovým rozlíšením záznamu 1 minúta. Ročné maximá intenzít dažďa boli vypočítané pre zvlášť každú lokalitu a pre všetky uvažované trvania dažďa. Vzhľadom na relatívne krátke časové rady (< 20 rokov) sme pri odhade parametrov GEV rozdelenia ročných maxím použili princíp bayesovskej inferencie. Lokálne odhady intenzít dažďa pre zvolené doby opakovania sme interpolovali v priestore, čím sme získali odhady návrhových intenzít dažďa aj pre lokality bez trvale inštalovaného zrážkomeru. Spomedzi metód opísaných v literatúre, ktoré sú použiteľné pre účely interpolácie staničných záznamov atmosférických zrážok do regularizovaného gridu, sme vybrali metódu trivariatného regularizovaného splajnu s tenziou (v.vol.rst). Táto interpolačná metóda je implementovaná v GIS prostredí GRASS. Trivariatný regularizovaný splajn s tenziou nám umožnil využiť informáciu o nadmorskej výške ako dodatočného kovariátu k zemepisnej šírke a dĺžke, čo nám umožnilo lepšie zohľadniť vplyv orografie na priestorové rozloženie návrhových hodnôt intenzít dažďa. Horizontálne rozlíšenie výsledných rastrových vrstiev s gridovanými návrhovými intenzitami dažďa je 500 metrov. Jednotlivé dátové polia obsahujúce návrhové intenzity dažďa pre jednotlivé doby opakovania boli zoskupené do jednej multidimenzionálnej kocky z ktorej môžeme extrahovať IDF krivky pre ľubovoľnú lokalitu na Slovensku. Za účelom ilustrovania priestorovej variability intenzít dažďa sme zahrnuli do tohto článku aj príklady máp intenzít dažďa. V blízkej budúcnosti plánujeme ako ďalší krok vytvoriť grafické rozhranie pomocou ktorého bude možné výsledky tejto štúdie operatívne používať ako technickú pomôcku v klimatologickej službe SHMÚ.

Key words: rainfall intensity, IDF, tri-variate regularized splines with tension, atlas

INTRODUCTION

Intense rainfall events deliver large amounts of rain water over short periods of time. Intense rains are capable of overwhelming storm drains, flood basements, wash out bridges and roads, and triggering floods and initiating landslides. To reduce the risk of damages to property, hydrologists, civil engineers and public authorities need accurate information about the probability of occurrence of extreme rainfall events (Bedient et al., 2008; Koutsoyiannis et al., 2004 a,b; Koutsoyiannis et al., 1998; Koutsoyiannis et al., 2022; Onderka and Pecho, 2022 a). Short-duration rainfall intensities, graphically displayed in the form of Intensity-Duration-Frequency (IDF) curves (or Depth-duration-Curves), are used by civil engineers in calculations of peak runoff for design of a variety of storm water management structures such as storm sewers, storm water detention structures (Bedient et al., 2008). IDF curves have been used in hydrology for almost a century now (Sherman, 1932). IDF curves gained their popularity due to their practical benefits when engineering problems are affected by rainfall extremes.

In Slovakia, the calculation of rainfall frequency estimates has historically been the responsibility of the national weather service (nowadays the Slovak Hydrometeorological Institute). Over time, several estimates of rainfall design values were published in different technical reports and research papers such as the early works of Dub (1946), Dzubák (1969), Šamaj and Valovič (1973), Urcikán and Imriška (1986), mostly using historical records from rain gauges at a limited number of locations. Attempts to establish regional curves based on the ergodic behavior of rainfall extremes were made by Kupčo (1985) and Kupčo et al. (2021). For example, Šamaj and Valovič (1973) analyzed pluviograms from 68 self-registering rain gauges with source data covering mostly the first half of the 20th century. More recent studies concerned covering this topic in Slovakia are the papers of Gaál et al. (2009), Bara et al. (2009), Kupčo et al. (2021), Onderka at al. (2020 a, b, 2022 a).

The concept of IDF curves is widely used in the design and evaluation of urban drainage infrastructure. The Slovak Technical Standard STN 75 6101 (2002) required the modified rational method to be used as the main design and evaluation method in Slovakia. This technical standard implicitly requires application of IDF curves in determining design (peak) flow for a specific sewer system section, depending on the travel time of a particular sub-catchment. The IDF relationships of Urcikán and Imriška (1986) were recommended by the aforementioned Slovak Standard STN 75 6101 (2002) for provisional plans. In 2018, the Slovak Technical Standard STN 75 6101 was replaced by the European standard STN EN 16933-2 (2018). However, this European standard also states, that the "relevant authority" can specify design rainfall values to be used, reflecting the local conditions, and that these values can be provided in the form of constant rainfall rates calculated from intensity-duration-frequency (IDF) curves. IDF curves are one of the basic design parameters used in the urban hydrology and urban drainage. Unfortunately, in Slovakia, parameters/values of the IDF curves have not been updated since 1986. It is a particularly unpleasant situation as many activities are underway (reconstruction of the existing urban drainage systems, as well as implementation of adaptation and mitigation measures for climate change in urbanized areas).

This paper builds upon our recent work that has been published within the National Climate Report of Slovakia (Onderka and Pecho, 2022a) that contains local estimates of rainfall intensities calculated for return periods up to 1000 years and rainfall durations from 5 minutes to 300 minutes. However, it is necessary to interpolate the local estimates in space so that the design values of rainfall intensities can be retrieved also for un-gauged locations. The goals of this paper are therefore:

(1) to briefly describe the computational framework we applied in estimating local (station-based) design values of rainfall intensities;
(2) to parameterize the locally established intensity-duration-frequency relationships;
(3) to interpolate local estimates rainfall intensities into a regular grid;
(4) to present illustrative graphical outputs in the form of maps showing the overall spatial variability of design values for selected return periods and rainfall durations from 5 minutes to 24 hours.

DATA AND METHODS

Processing rainfall data

Data from a total of 183 rain gauges with 1-minute temporal resolution were processed. The period of time over which the rainfall data were processed ranges from 1991 to 2021, although some variability in the length of the time series exists between the individual rain gauges due to gaps in the time series. Rainfall was registered by two types of rain gauges, automatic instruments with capture area of 200 cm^2 (TRws 214 manufactured by MPS system Ltd.) and mechanical self-registering rain gauges with capture area of 250 cm^2 (METRA manufactured in the former Czechoslovakia). The exact locations of the rain gauges are shown in Fig. 1. First, raw 1-minute series of rainfall were screened for basic quality issues (identification of gaps, instrument

Figure 1. Map showing the study region and the locations of self-registering rain gauges (WGS84 projection).

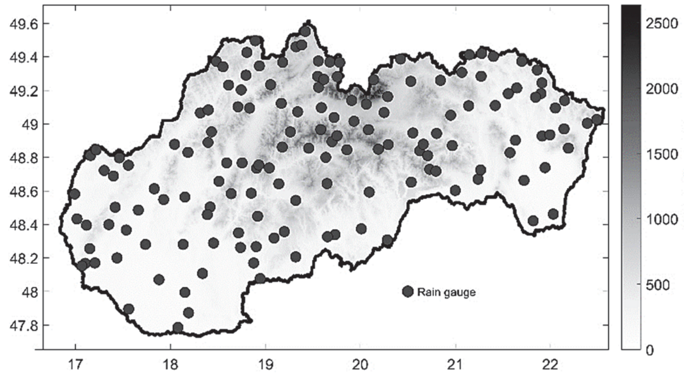

failure, outliers etc.). Subsequently, the 1-minute data were aggregated to intensities with rainfall durations of 5, 10, 15, 20, 30, 40, 50, 60, 90, 120, 180, 240, 300, 360 … 1440 minutes. Annual maxima of rainfall intensities were calculated for data from the warm part of the year (i.e. April to October). Suspicious data in the annual maxima series (based on a threshold) were visually inspected by plotting a short sequence of rainfall observations prior to and after a spurious value. Erroneous data were removed from the time series. For locations where both the automatic and mechanical self-registering rain gauges were in operation, their annual maxima were combined in order to achieve longer time series. The resulting number of unique locations is therefore 150. A more detailed description of the rain gauge data is provided in the National Climate Report of Slovakia (Onderka and Pecho, 2022a).

IDF relationship

A rainfall frequency estimate for a given location is defined as the intensity of rainfall for a specific duration that has a certain return period. When rainfall intensities are calculated for a range of durations and frequencies (return periods), the resulting set of curves are referred to as intensity-duration-frequency curves, also known in their abbreviated form as IDF curves. As Koutsaiannis and Iliopoulou (2022) recently noted, the term "IDF curve" is a misnomer. Instead of using duration, time scale of averaging is a more appropriate term, and frequency should be preferred to return period. Nevertheless, we stick with the traditional term in this paper. A new term "*ombrian curve*" (from the Greek word "*ombros*", meaning rain in English) has been suggested for the mathematical relationship between average rainfall intensity, time scale of averaging and return period. Construction of IDF curves can follow two different approaches: local station-based independent fitting approach, which consists of separately fitting the curves to multiple gauged sites and using spatial interpolation methods to map the parameters in space; or the regional approach based on appropriately pooling the data together and obtaining a single model valid over the entire area of interest. Frequency of occurrence of a rare event can be defined in terms of annual exceedance probability or average return period. Annual exceedance probability is a probability associated with exceeding a given rainfall intensity for a specified duration at least once a year. For instance, a return period of 100 years is the average time between exceedances of a given intensity for a specified duration.

GEV distributions of rainfall intensities

Several methods have been developed that can be used to estimate GEV parameters: probability-weighted moments, maximum likelihood estimation (MLE), and Bayesian inference (Onderka et al., 2022 a, b; Coles, 2001). The Bayesian inference of distribution parameters is used in this paper, for it has previously proven to be robust against the issues of short time series (Coles, 2001; Onderka and Pecho 2022 a, in press). The GEV distribution is used here to model annual maximum rainfall intensities. The cumulative distribution function $G(x)$ for the GEV distribution is given as:

$$G(x) = \exp\left[-\left(1+\xi\left(\frac{x-\mu}{\sigma}\right)\right)^{-1/\xi}\right], \quad (1)$$

where μ is the location parameter indicating where the extremes distribution is centered, σ is the scale parameter specifying the deviations around μ, and ξ is the shape parameter describing the tail behavior of the GEV distribution (Coles, 2001; Ragno et al., 2019; Cheng et al., 2014, 2015; Koutsoyiannis et al., 2004 a,b). In its limit form when $\xi \rightarrow 0$, the GEV distribution corresponds to the Gumbel distribution, for $\xi < 0$ to the Weibull distribution, and for $\xi > 0$ with the Fréchet distribution (Coles, 2001), but this notational convention is not always followed in hydrology. If we know the parameters of $G(x)$ than the estimated values of the extreme quantiles of annual maxima can be determined from the inverse function (2):

$$x = \begin{cases} \mu - \frac{\sigma}{\xi}[1 - \{-\log(1-p)^{-\xi}\}] & for\ \xi \neq 0 \\ \mu - \sigma \log\{-\log(1-p)\} & for\ \xi = 0, \end{cases} \quad (2)$$

where x is the quantile of rainfall intensity corresponding to the return period T. The x quantile can therefore be thought of as an intensity that is expected to be exceeded on average every T years, Alternatively, one may say that the rainfall intensity is exceeded in every single year with a probability *p*.

Bayesian inference of GEV parameters

Let $\boldsymbol{\theta}$ be a vector with parameters of a distribution function and $\boldsymbol{y} = \{y_1, \ldots, y_m\}$ is another vector with observations, which can be a sequence annual maxima of rainfall intensities observed over *m* years. In Bayesian inference we use *a priori* likelihood of model parameters, i.e. probability density function of $p(\boldsymbol{\theta})$, in practice also commonly described as the *prior.* On the other hand, a posterior density function (*posterior*) $p(\boldsymbol{\theta}\,|\,\boldsymbol{y})$ reflects our knowledge of a how a model behaves with the help of a *prior* and a *likelihood function* of observed data $p(\boldsymbol{y}½\boldsymbol{\theta})$. From the Bayesian theorem (3) it follows that the probability of model parameters $\boldsymbol{\theta}$ conditioned by observations $\boldsymbol{y}$, *i.e. the posterior* $(\boldsymbol{\theta}\,|\,\boldsymbol{y})$ proportionally increases with $\boldsymbol{\theta}$ (*prior*) and the probability of observations $\boldsymbol{y}$ conditioned by the parameters $\boldsymbol{\theta}$, *i.e.* $p(\boldsymbol{y}\,|\,\boldsymbol{\theta})$:

$$p(\boldsymbol{\theta} \mid \boldsymbol{y}) \propto p(\boldsymbol{\theta}) \ \prod_{i=1}^{n} p(y_i \mid \boldsymbol{\theta}), \quad (3)$$

where $\propto$ is the symbol of proportionality and $\prod_{i=1}^{n} p(y_i \mid \boldsymbol{\theta})$ is the likelihood function (Onderka et al., 2022a; Agha-Kouchak et al., 2013; Coles, 2001; Ragno et al., 2019). Each parameter of the GEV distribution (μ, σ, ξ) has its own prior which values should be chosen on the basis of theoretical or empirical *a priori* knowledge. In cases when only a limited amount of data are available (e.g. short time series of rainfall data), the prior significantly affects the posterior.

Prior distribution

The choice of every parameter of the GEV distribution has a great impact on the distribution of the inferred quantile of rainfall intensities (posterior) especially in cases when we do not have a sufficiently long time series of observations. The shape parameter ξ dictates the behavior of the "*heavy tails*" of the distribution function containing rainfall extreme values. Koutsoyiannis et al, (2004a, 2004b) provided theoretical and empirical proofs that the commonly used Gumbel distribution (i.e. where $\xi \to 0$) is not a suitable option for analyzing rainfall extremes. In specifying the prior distribution for the shape parameter ξ we relied on the research of Ulrich et al. (2021), Lutz et al. (2020), Papalexiou and Koutsoyiannis (2013), Koutsoyiannis et al. (2004 a, b) and Serinaldi and Kilsby (2014). Ulrich et al. (2021) estimated that the shape parameter ξ is as a function of rainfall duration from 1 minute to 120 hours with values ∈ (0; 0, 3). On the basis of these studies we chose the prior of the shape parameter $\xi \in N(0.15;\ 0.075)$, where 0.15 je the mean and 0.075 is standard deviation. Since the physical nature of rainfall intensities restricts the prior of the location parameter μ to be $\in N\{\text{mean}(y);\ \text{StDev}(y)\}$. The scale parameter σ was modelled in logarithmic scale, as described in Coles (2001) and Ragno et al. (2019). The prior of the scale parameter was defined to be within $\sigma \in N(0;\ 10)$. The Markov Chain Monte Carlo (MCMC) method was deployed to derive estimates of the model parameters $\boldsymbol{\theta}$ yielding a large sample of model parameters that can be considered as realization from the posterior distribution $p(\boldsymbol{\theta}\,|\,\boldsymbol{y})$. A detailed description of how we estimated the marginal distribution of the GEV parameters by using an MCMC sampler on sample data from the Hurbanovo station (Slovakia) can be found in our recently published paper (Onderka et al., 2022b).

Empirical intensity-duration-frequency relationships

Relationships between rainfall intensity, duration and frequency of occurrence can be graphically represented as IDF curves (Koutsoyiannis et al., 1998). The mathematical relationship between rainfall intensity i, duration D can be empirically expressed for each return period T (Koutsoyiannis et al., 1998):

$$i(D,T) = \frac{\lambda}{(D+\delta)^{\eta}}, \tag{4}$$

where D (min) is the duration, and λ, δ, η are empirical parameters. Eq. 4 is also known as the Sherman equation (Sherman, 1932). At the same time, the following restricting conditions apply for η and δ: $0 < \eta \leq 1$ a $\delta \geq 0$. It is obvious, that the equation does not have an analytical solution. Therefore, we estimated its three parameters (λ, δ, η) by using the *Levenberg-Marquardt* optimization technique, where the minimum of mean squared error was used as the objective function. For each location (rain-gauge) separately, a set of IDF curves was fitted to rainfall quantiles (q_s) corresponding to return periods $T = 2$–100 years and durations D ranging from 5 to 1440 minutes.

Spatial interpolation of IDF parameters and rainfall design values

In this paper, we used the "*v.vol.rst*" package implemented within GRASS (Geographic Resources Analysis Support System). This package interpolates values from a 3-dimensional field of points to an interpolated 3-dimensional raster map. As we are interested in a 2-dimensional map showing the spatial variability of rainfall intensities, it is desirable taking a cross-sectional surface from the 3-D raster map. Specifying cross-input and cross-output option, one gets the output 2D raster map containing the cross-section of the interpolated volume with a surface defined by cross-input 2D raster map. The tension parameter controls the distance over which each given point influences the resulting volume. When the tension parameter is set to a high values, each grid point is affected only by the closest grid points. Higher values of the tension parameter reduce overshooting (Hofierka et al., 2002; Mitašová and Mitaš, 1993). For noisy data, it is possible to define a global smoothing parameter. With the smoothing parameter set to zero (smooth = 0) the resulting volume passes exactly through the data points. A spline function $S(\boldsymbol{x})$ is obtained by minimizing the deviation from the vector of observed data and the smoothness seminorm $I(S)$:

$$\sum_{j=1}^{N}\left|p^{[j]} - S(\boldsymbol{x}^{[j]})\right|^2 w_j + w_0 I(S) = minimum, \tag{5}$$

where $r^{[j]}$ are the observations of rainfall intensities made at discrete points (rain gauges) $\boldsymbol{x}^{[j]} = (x_1^{[j]}, \ldots x_d^{[j]})$, $j = 1,\ldots, N$ within a region of a d-dimensional space, and where w_j and w_0 are weights and $I(S)$ is the smooth seminorm. In the case when $w_0/w_j = 0$ the spline function $S(\boldsymbol{x})$ passes exactly through the observed data points. This minimization problem (Eq, 1) is a sum of a trend function $T(\boldsymbol{x})$ and a *radial basis function* $R(\boldsymbol{x}, \boldsymbol{x}^{[j]})$:

$$S(\boldsymbol{x}) = T(\boldsymbol{x}) + \sum_{j=1}^{N} l_j R(\boldsymbol{x}, \boldsymbol{x}^{[j]}). \tag{6}$$

First, we need to define a tri-variate RST function, For N observations of rainfall $r^{[j]}$ at discrete points in space $\boldsymbol{x}^{[j]} = (x_1^{[j]}, \ldots x_d^{[j]})$ the tri-variate function can be written as:

$$r = F(x_1, x_2) = S(x_1, x_2, cG(x_1, x_2)), \tag{7}$$

where c is a vertical scaling parameter, S is the tri-variate RST function.

The tension, smoothing and vertical scaling parameters in Eq. 7 can be chosen based on experience or by minimizing an objective function (*e.g.* the mean absolute error - MAE or the root mean square error - RMSE). It is important to note that the resolution and smoothing of the covariate (in our case the DEM model) impact the resulting spatial pattern of the gridded data crossing the intersection surface $G(x_1, x_2)$ and thus the spatial variability of the interpolated map of rainfall intensities $p = F(x_1, x_2)$. A detailed mathematical description is in the papers of Hofierka et al. (2002), Mitašová and Mitaš (1993). For the purposes of this paper, we used the *jack-knife* cross-validation procedure to evaluate the predictive accuracy of the RST function.

Using the *jack-knife* method, every point representing a rain-gauge location was temporarily excluded from the computation and interpolation error for this point location were computed. As a covariate in the RST function, we used the DEM with 500-horizontal resolution (JTSK03/Krovak projection - EPSG code: 8352). We used the "*v.vol.rst*" package to interpolate the IDF parameters (Eq. 4) and the local rainfall quantiles estimated for 150 locations (Eq. 2). As a result, we created 224 arrays of rainfall intensities corresponding to 2 – 100 year return *T* periods and durations *D* from 5 to 1440 minutes (7×32=224).

The general concept of the multidimensional array of IDF relationship is depicted Fig. 2. The whole idea of using such an array is to extract rainfall quantiles for chosen durations *D* at any location in Slovakia.

Figure 2. Schematic description of IDF extraction from a multidimensional array with rainfall intensities corresponding to chosen durations D and return periods T.

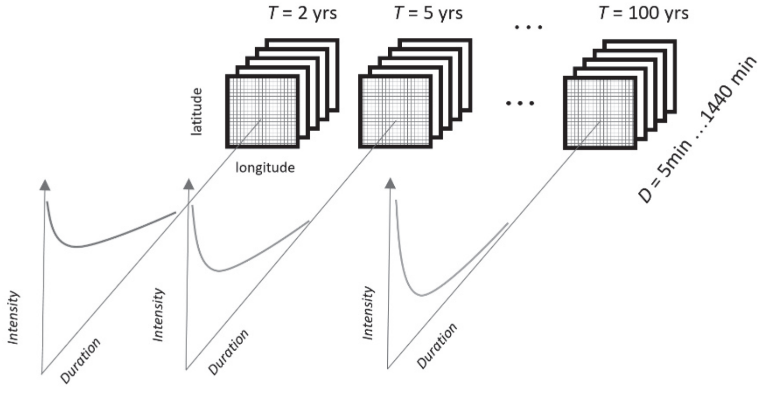

Figure 3. IDF curves derived for the Bratislava - Koliba location [Rain gauge ID 17140; longitude: 17.10611, latitude: 48.16778, altitude: 283 m]. Only durations from 5 to 180-minutes are shown for return periods T = 2, 5, 10, 20, 30, 50 and 100 years.

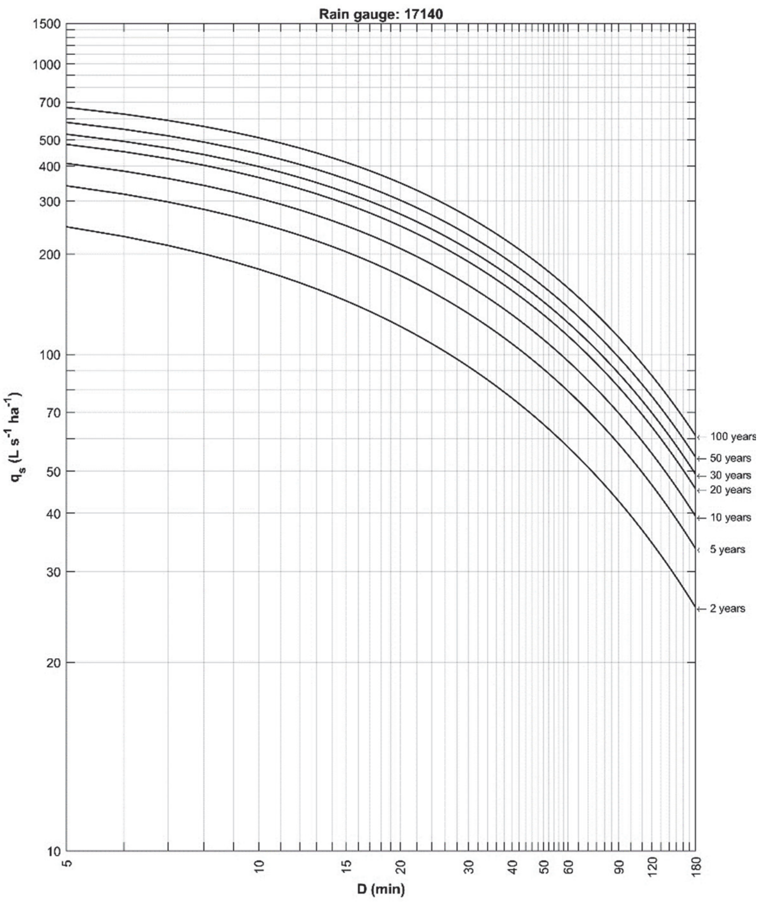

RESULTS

Local IDF curves

To give an example of a set of station-based IDF curves we have plotted IDFs derived from rainfall data observed at the Bratislava - Koliba station in Fig. 3. To annual maxima series at this station cover the period 1995 – 2015.

To show the overall behavior of IDF curve parameters a statistical summary of the derived IDF parameters (λ, δ, η) over all rain gauges is indicated in Tab. 1. The median value of the λ parameter in Eq. 4 has an increasing tendency with return period (Tab. 1) with a value of 1973.33 for 2-year return period and up to 6591.66 for the 100-year return period. On the other hand, the remaining parameters δ and η do not seem to change considerably across the considered return periods. To illustrate a common shape of IDF curves the individual IDF curves generated for all 150 locations were pooled. The 2-year return period was chosen for an illustration (Fig. 4). Summary statistics on the underlying IDF curves was calculated. As shown in Fig. 3, the curve tapers off at durations below approx. 180 minutes. Above this "limit", the IDF curves appear as straight lines in the log-log space (Fig. 3).

IDF envelope curves

As an upper bound of the derived IDF relationships across the whole territory of Slovakia we pooled the individual design values calculated for the 150 locations and calculated the 95th percentile for each duration *D* and return period *T* (Tab. 2). Fig. 4 illustrates an ensemble of intensity-duration relationships for the return period *T* = 2 years. Despite chosen arbitrarily, the 95th quantile approximates the concept of envelope curves. For the purposes of this paper an envelope curve is broadly defined as an upper percentile, i.e. the 95th percentile calculated of all values. Šamaj and Valovič (1973, page 28) used station-based rainfall intensities to construct a single envelope curve for the whole territory of Slovakia. We compared the 95th percentiles calculated in our study (Tab. 2) with the maximum intensities (Tab. 3) that were calculated in the past by Dub (1946) and Šamaj and Valovič (1973). For instance, the previously reported 5-minute rainfall intensities of 883 L.s^{-1}.ha^{-1} (Šamaj and Valovič, 1973) and 900 L.s^{-1}.ha^{-1} (Dub, 1946) correspond with the 30 to 50-year intensities (Tab. 2). For duration D = 10… 120 minutes the maximum intensities observed in the past correspond to the return period 50 – 100 years.

Interpolated IDF parameters and design values of rainfall

The mean absolute error (MAE) was used to optimize the choice of parameters in the RST interpolation model (tension, smoothing and vertical scaling). The MAE measured differences between predicted (interpolated) values and the actually observed values (local estimates of quantiles). Tab. 4 shows the minimized MAE values calculated by the *jack-knife* (leave-one-out resampling) method. To assess the performance of the interpolation model, the local quantiles are plotted against the interpolated values (Fig. 5). Although shown only for hourly and sub-hourly durations, the coefficient of determination R^2 is above 0.9 and tends to increase with the duration D.

The interpolated parameters λ, δ, η of the IDF relationship (Eq. 5) are depicted in Fig. 6 – 8. Although these interpolated parameters were not further used in the calculations of quantiles for un-gauged locations, the spatial pattern of these parameters shows the complexity of IDF relationships. Finally, the interpolated local quantiles of rainfall design values are presented in Fig. 9 – 13.

Table 1. Descriptive statistics of the IDF parameters (n = 150).

T (years)	2	5	10	20	30	50	100
			***λ* parameter**				
Minimum	958.33	1258.33	1430.00	1636.67	1765.00	1921.67	*2085.00*
Maximum	5536.66	9928.33	14286.66	18031.66	20343.33	23414.99	*27894.99*
Median	**1973.33**	**3041.67**	**3836.67**	**4658.33**	**5088.33**	**5695.00**	***6591.66***
St.Dev	846.67	1583.33	2231.67	2835.00	3195.00	3670.00	*4351.66*
			***δ* parameter**				
Minimum	0.83	0.00	0.00	0.00	0.00	0.00	*0.00*
Maximum	17.53	23.92	30.82	35.15	37.31	39.76	*42.67*
Median	**6.39**	**7.12**	**7.32**	**7.34**	**7.37**	**7.39**	***7.60***
St.Dev	3.16	4.31	5.07	5.62	5.90	6.21	*6.58*
			***η* parameter**				
Minimum	0.66	0.67	0.66	0.66	0.67	0.67	*0.67*
Maximum	0.99	0.99	0.99	0.99	0.99	0.99	*0.99*
Median	**0.84**	**0.86**	**0.86**	**0.87**	**0.87**	**0.88**	***0.88***
St.Dev	0.06	0.07	0.08	0.08	0.08	0.09	*0.09*

Table 2. Envelope-curve generating data (95th percentile) obtained from local IDF curves (n = 150 locations). Intervals covering the maximum intensities of Dub (1946) and Šamaj and Valovič (1973) are indicated in bold (printed in bold).

T (years)		2	5	10	20	30	50	100
***D* (min)**	**5**	333.97	494.94	618.85	743.57	**821.80**	**928.93**	1083.04
	10	244.30	345.27	424.87	518.06	573.43	**638.97**	**739.97**
	15	194.36	273.02	332.75	400.06	443.36	**496.62**	**577.22**
	20	162.31	228.79	280.06	333.70	368.10	**412.00**	**478.05**
	30	123.59	175.19	216.30	260.28	285.86	**320.32**	**371.56**
	40	100.97	142.06	176.61	212.20	233.15	261.53	**302.67**
	50	85.49	121.07	150.06	177.77	195.36	219.49	**256.90**
	60	73.81	105.47	129.69	154.84	170.72	192.26	**224.57**
	90	52.59	76.24	94.13	113.55	124.56	139.69	**162.72**
	120	41.93	60.23	74.73	91.05	99.95	111.32	**129.44**
	180	30.58	43.80	54.59	65.82	72.62	81.70	95.08
	240	24.39	34.61	43.07	51.96	57.49	64.77	75.73
	300	20.43	28.68	35.61	42.86	47.66	53.67	62.97
	360	17.58	24.80	30.62	37.15	41.21	46.30	53.94
	420	15.49	22.03	27.14	32.91	36.51	41.08	47.60
	480	13.89	19.96	24.62	29.63	32.87	36.99	42.88
	540	12.64	18.32	22.59	27.00	29.96	33.67	39.11
	600	11.69	16.87	20.95	24.85	27.57	30.95	36.02
	660	10.87	15.57	19.56	23.07	25.57	28.68	33.44
	720	10.13	14.44	18.18	21.66	23.94	26.81	31.24
	780	9.50	13.46	16.93	20.44	22.53	25.24	29.39
	840	8.97	12.68	15.87	19.29	21.30	23.88	27.80
	900	8.51	12.04	15.06	18.21	20.22	22.67	26.41
	960	8.10	11.47	14.36	17.36	19.23	21.40	25.00
	1020	7.72	10.96	13.72	16.56	18.33	20.43	23.71
	1080	7.38	10.50	13.15	15.82	17.51	19.60	22.61
	1140	7.07	10.09	12.64	15.15	16.78	18.84	21.68
	1200	6.79	9.71	12.16	14.55	16.11	18.15	20.87
	1260	6.53	9.38	11.73	13.99	15.49	17.51	20.13
	1320	6.30	9.09	11.26	13.48	14.93	16.87	19.46
	1380	6.09	8.79	10.82	13.01	14.41	16.29	18.84
	1440	5.90	8.52	10.42	12.57	13.93	15.75	18.26

Table 3. Maximum rainfall intensities in Slovakia calculated in the past by O. Dub (1946) and Šamaj and Valovič (1973).

	D(min)	5	10	15	20	30	60	90	120
O. Dub (1946)	*i* (L.s^{-1}.ha^{-1})	900	637	510	431	325	200	145	120
Šamaj and Valovič (1973)	*i* (L.s^{-1}.ha^{-1})	883	680	550	466	366	238	180	146

Figure 4.
Ensembled Intensity-Duration relationships generated for return period T = 2 years. The descriptive statistics is based on the individual Intensity-Duration relationship (n = 150 locations). A slight tapering of the curve is present at durations D below approximately 180 minutes.

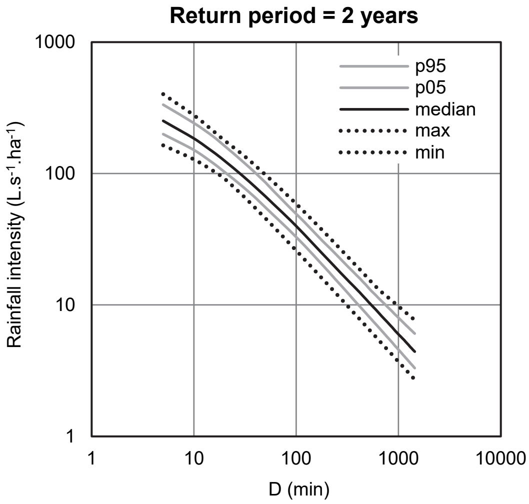

Figure 5. Cross-validation of local rainfall intensities versus interpolated rainfall intensities (n = 150) for: (A) 5-minute durations; (B) 15-minute durations; (C) 30-minute durations; and (D) 60-minute durations.

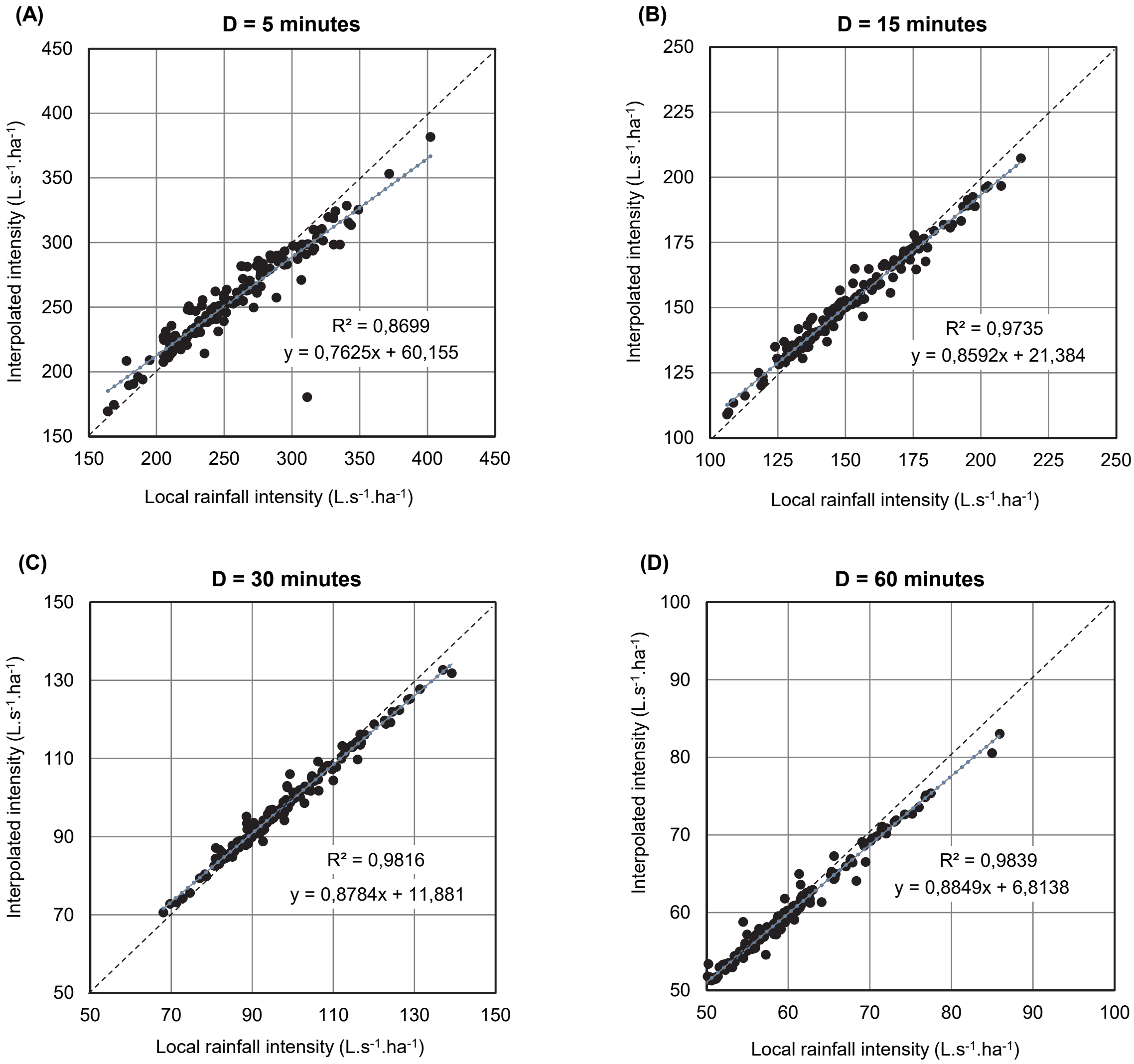

Table 4. Mean absolute errors – MAE ($L.s^{-1}.ha^{-1}$). MAE was calculated by the jack-knife (leave-one-out resampling) method (n = 150).

D (min) \ *T* (years)	2	5	10	20	30	50	100
5	44.3197	79.7213	106.8560	135.5110	153.0290	176.1240	336.9060
10	23.0248	46.4670	63.3801	81.5755	92.7252	107.2990	206.7940
15	16.6696	33.8471	46.5480	59.9005	68.0951	78.9484	153.2820
20	13.4605	24.1543	37.3007	48.2313	54.9493	63.7492	124.8760
30	9.9024	17.5667	24.5930	32.2739	40.3967	47.0540	93.4188
40	7.9070	14.0826	19.6038	25.7554	29.5837	34.6667	75.1927
50	6.6389	11.8084	16.3503	21.4807	24.6927	28.9711	63.1964
60	5.7546	10.2287	14.2129	18.6702	21.4627	25.1809	54.9841
90	4.1890	7.3932	10.2198	13.4053	15.4094	18.0753	37.4345
120	3.3616	5.8778	8.1123	10.5622	12.1361	14.2322	29.6392
180	2.4922	4.3493	5.9662	7.7257	8.8346	10.3071	21.3996
240	2.0455	3.5505	4.8421	6.2398	7.1173	8.2875	16.9629
300	1.7741	3.0403	4.1392	5.3152	6.0430	7.0344	14.3298
360	1.5793	2.6783	3.6275	4.6558	5.2827	6.1269	12.4960
420	1.4357	2.4247	3.2702	4.1952	4.7554	5.5123	11.2090
480	1.3180	2.2174	2.9796	3.8118	4.3230	5.0079	10.1584
540	1.2227	2.0507	2.7520	3.5109	3.9759	4.6007	9.3433
600	1.1473	1.9234	2.5809	3.2922	3.7284	4.3127	8.7605
660	1.0806	1.8067	2.4214	3.0879	3.4974	4.0440	8.1876
720	1.0275	1.7191	2.3028	2.9404	3.3300	3.8494	7.7822
780	0.9781	1.6323	2.1824	2.7886	3.1586	3.6538	7.3605
840	0.9383	1.5668	2.0968	2.6815	3.0383	3.5180	7.0684
900	0.9000	1.4978	2.0049	2.5647	2.9058	3.3648	6.7371
960	0.8703	1.4480	1.9428	2.4843	2.8161	3.2599	6.5198
1020	0.8396	1.3928	1.8683	2.3884	2.7077	3.1342	6.2582
1080	0.8215	1.3679	1.8383	2.3495	2.6648	3.0828	6.1505
1140	0.7962	1.3233	1.7760	2.2689	2.5735	2.9766	5.9343
1200	0.7803	1.2973	1.7403	2.2204	2.5174	2.9097	5.7787
1260	0.7585	1.2591	1.6881	2.1526	2.4407	2.8207	5.6025
1320	0.7423	1.2326	1.6513	2.1052	2.3857	2.7569	5.4564
1380	0.7232	1.1994	1.6059	2.0469	2.3196	2.6799	5.3050
1440	0.7053	1.1684	1.5635	1.9924	2.2577	2.6081	5.1637

Figure 6. Spatial patterns of the λ parameter in the IDF relationship (Eq. 4) estimated for return period T = 10 years.

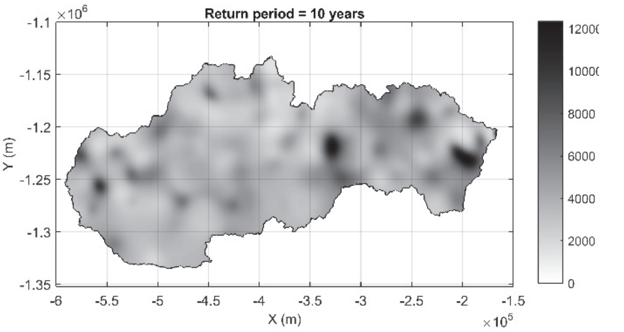

Figure 7. Spatial patterns of the δ parameter in the IDF relationship (Eq. 4) estimated for return period T = 10 years.

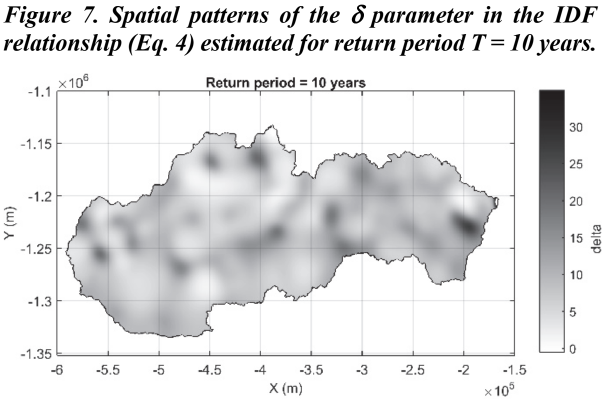

Figure 8. Spatial patterns of the η parameter in the IDF relationship (Eq. 4) estimated for return period T = 10 years.

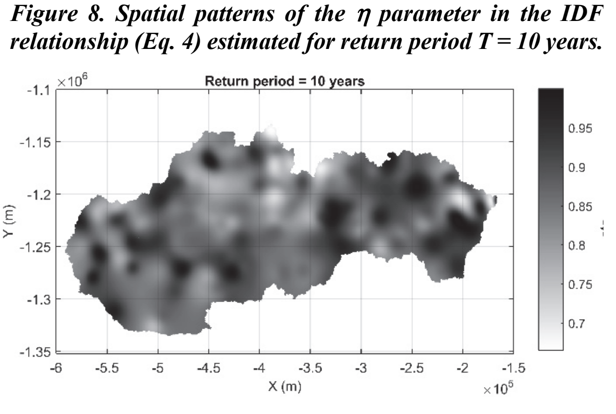

Figure 9. Maps of 5-minute rainfall intensities with return period T = 2, 5, 20, 100 years.

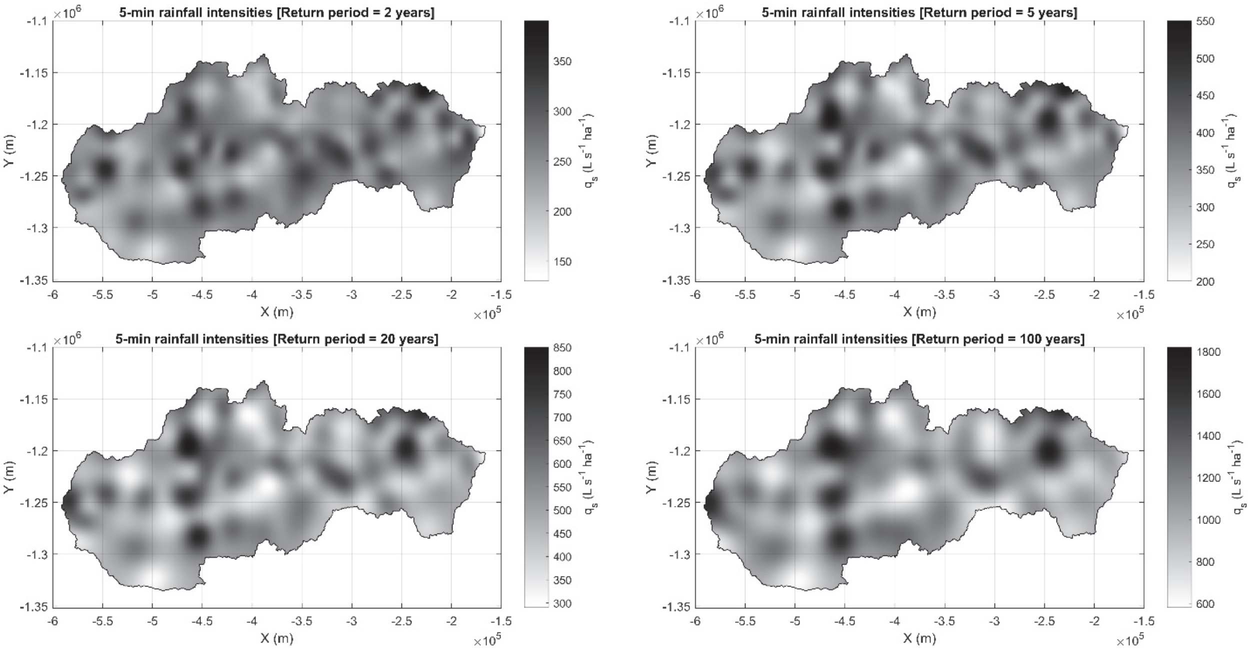

Figure 10. Maps of 15-minute rainfall intensities with return period T = 2, 5, 20, 100 years.

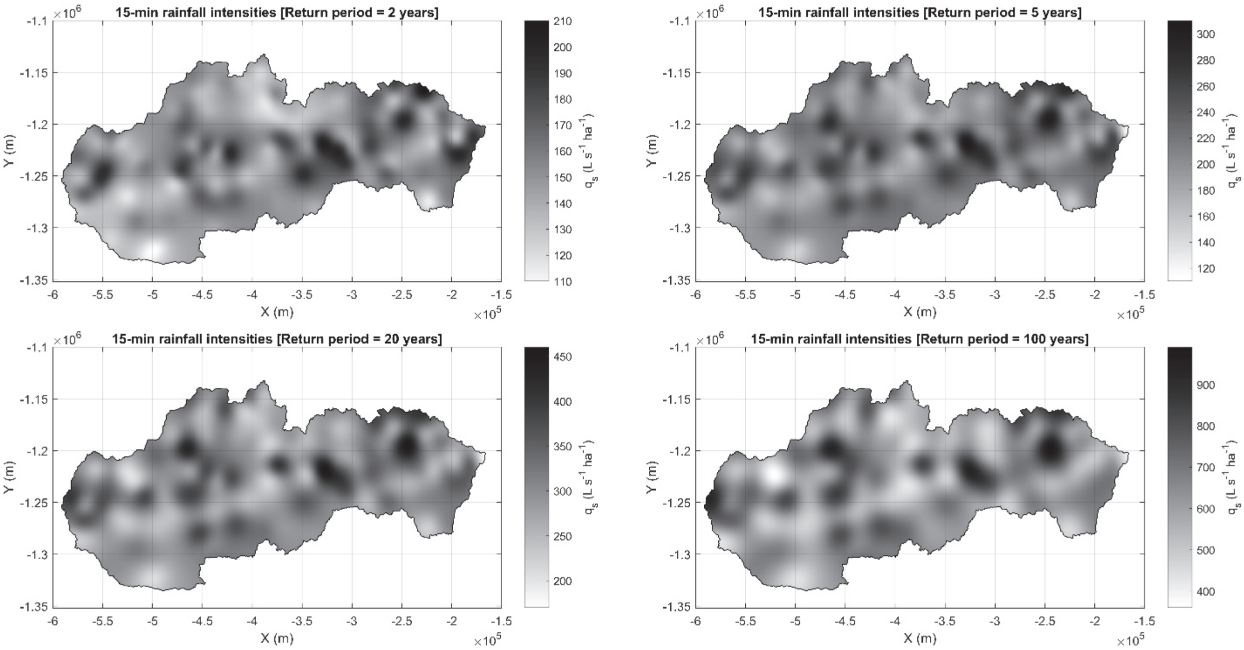

Figure 11. Maps of 30-minute rainfall intensities with return period T = 2, 5, 20, 100 years.

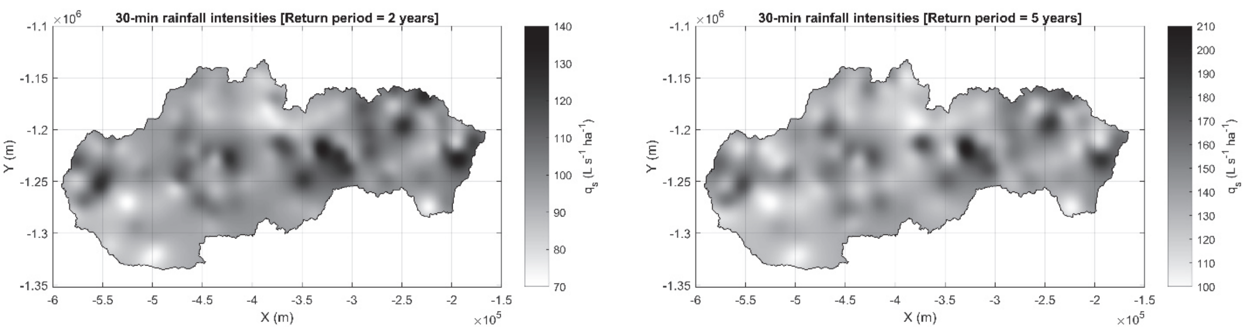

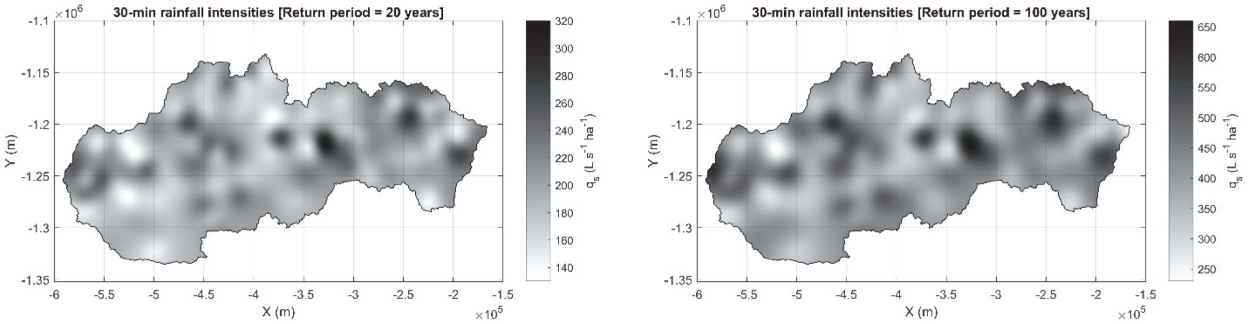

Figure 12. Maps of 60-minute rainfall intensities with return period T = 2, 5, 20, 100 years.

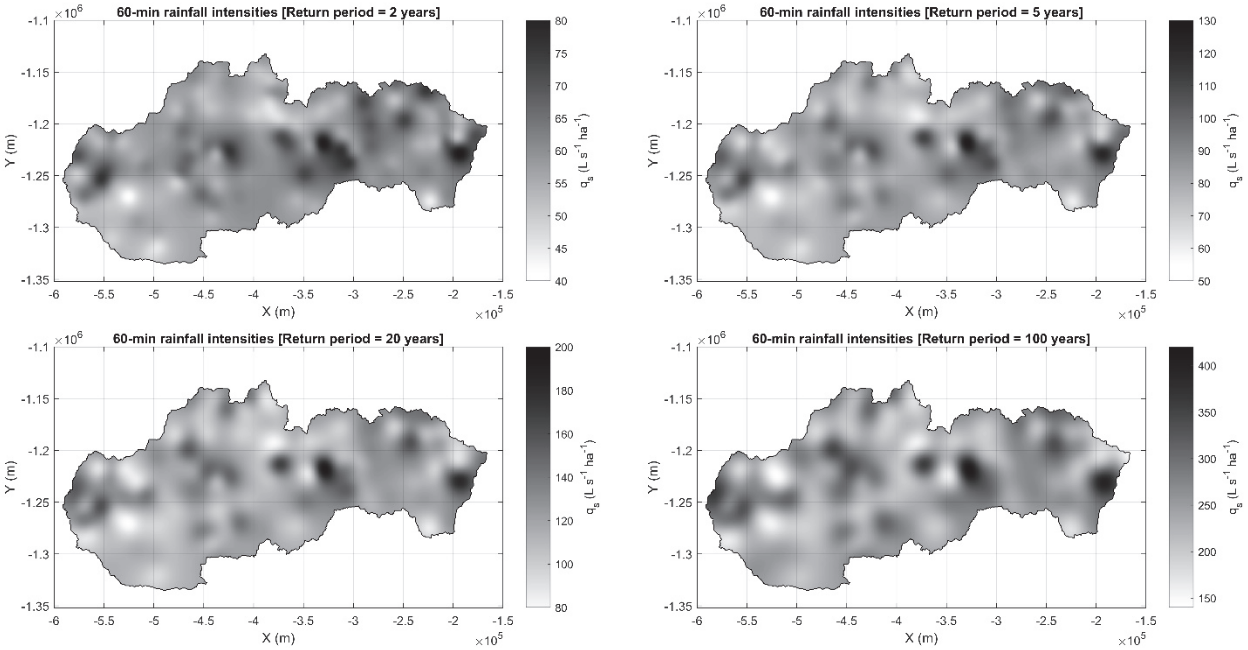

Figure 13. Maps of 360-minute rainfall intensities with return period T = 2, 5, 20, 100 years.

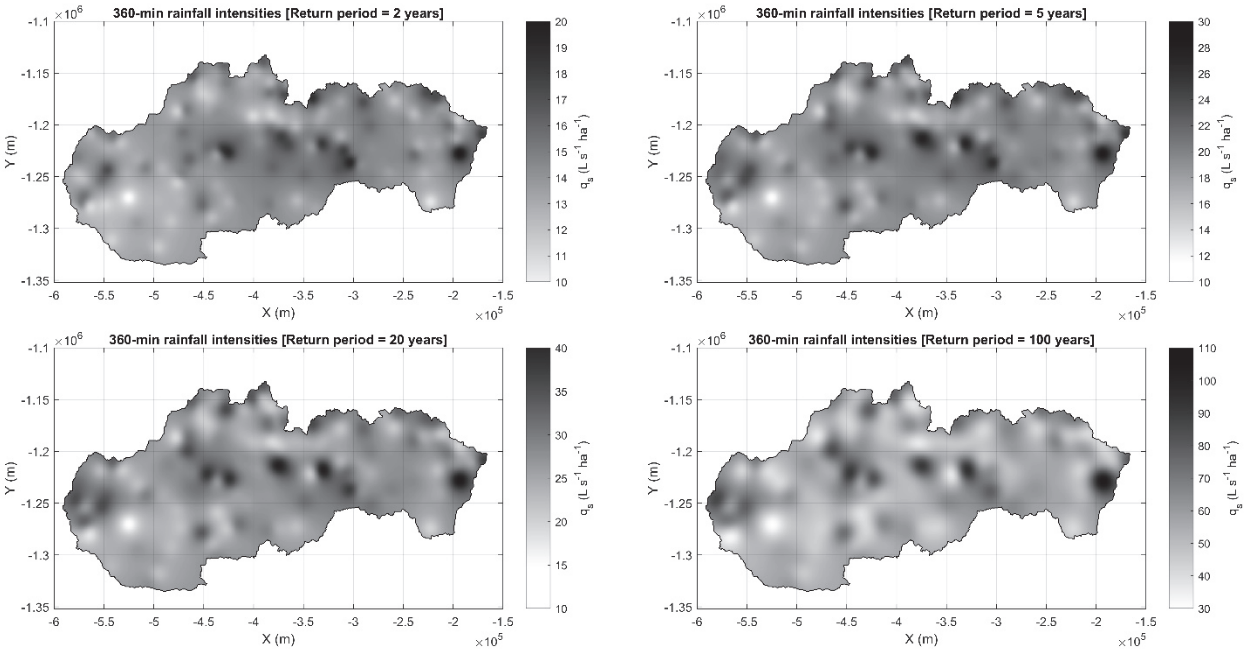

DISCUSSION AND CONCLUSIONS

Previous works concerned with IDF curves in Slovakia are rather outdated and may not necessarily serve their purpose anymore. In this study, we introduced an updated set of IDF curves using the most recent data covering the period between 1990 and 2020. The horizontal resolution of the resulting maps of gridded rainfall frequencies is 500 meters. Orography has a dominant effect on the dynamics of precipitation in the investigated region of Slovakia (Briedoň, 1961). Orographic effects, particularly the positive relationship between elevation and rainfall total over large temporal scales (hourly, daily, monthly, annual) have been widely studied. On the daily or hourly time scale, precipitation-elevation gradients are more complicated as differences in meteorological conditions due to static stability, flow direction and strength, freezing level between individual precipitation events dictate the variations of the precipitation-elevation relationship (Haiden and Pistotnik, 2009). To incorporate the effects of orography on the spatial pattern of rainfall intensities we applied the regularized spline with tension approach (Mitašová and Mitaš, 1993; Hofierka et al., 2002). A DEM model was used as a covariate to interpolate the locally estimated design values of rainfall intensities. This helped us to take into account the effects of orography on rainfall intensities. Consequently, local estimates of intensities have been determined for locations without rain gauges. It remains an interesting avenue for our future research to investigate the effects of orographic barriers on rainfall intensities on the leeward and windward slopes of mountains, valleys and mountain ridges. Rainfall extremes may increase in the future due to the elevated water capacity of the atmosphere (Onderka et al., 2020a, 2021). The individual layers have been stacked into a multidimensional cube from which we can abstract IDF curves specifying the requested return level for any location within the territory of Slovakia. Examples displaying the derived raster maps illustrate the spatial variability of rainfall intensities. It is necessary to create a user-friendly graphical interface in order to facilitate the use of the presented work by the climatological service of the Slovak Hydrometeorological Institute. Because the IDF curves are computed using historical observations of rainfall, our plan is to update the herein presented IDF relationships on a regular basis to reflect any changes in rainfall extremes in the future. We are convinced that the updated IDF curves will be beneficial especially for the community of civil engineers. As mentioned in the introduction section, the last update of IDF curves in Slovakia was made in 1986 (Urcikán and Imriška, 1986). Over the past decades, the total number of mechanical self-registration rain gauges increased, and additional automatic rain gauges have been installed throughout the entire territory of Slovakia. Climate change is another important reason to update the rainfall frequency estimates for the entire territory of Slovakia (Onderka and Pecho, 2021). Creating an atlas of IDF curves is a highly relevant task particularly for design of hydraulic infrastructure and evaluation of its hydraulic capacity, prevention of flooding events in urban areas, and eventually also for adaptation and mitigation measures in urban catchments. In the near future, an amendment to the Council Directive 91/271/ EEC of 21 May 1991 concerning urban waste-water treatment is underway. This amendment shall include a comprehensive assessment of wastewater management in urbanized areas, which should be reflected in the development of the Integrated urban wastewater management plans, which will be focused on initial situation analysis, definition of the objectives for the pollution reduction from storm water overflows (combined sewer overflows - CSO's) as well as the measures to be taken. We anticipate that this atlas will be appreciated especially by stake-holders involved in the ongoing Integrated urban wastewater management plans involving up to about 80 cities in Slovakia.

Acknowledgement

The research presented in this paper would not be possible without the following grants: *Scientific support of climate change adaptation in agriculture and mitigation of soil degradation* (ITMS2014 + 313011W580), supported by the Integrated Infrastructure Operational Programme and funded by the ERDF, and the national VEGA grant no. 2/0003/21 "*Complex analysis of the effects of rising air temperature on rainfall extremes in Slovakia*."

REFERENCES

AghaKouchak, A.–Easterling, A. et al., 2013, Extremes in a Changing Climate: Detection. Analysis and Uncertainty. Dordrecht: Springer. ISBN 978-94-007-4479-0.

Bara, M.–Kohnová S.–Gáal, L.–Szolgay, J.–Hlavčová, K., 2009, Estimation of IDF curves of extreme rainfall by simple scaling in Slovakia. Contributions to Geophysics and Geodesy. Vol. 39, 187–206. ISSN 1338-0540.

Bedient, P.–Huber, W.–Vieux, B., 2008, Hydrology and Floodplain Analysis: International Edition. 4th ed. Pearson Education (US). ISBN: 9780132422864.

Briedoň, V., 1961, Príspevok k závislosti zrážok od nadmorskej výšky v československej oblasti Karpát. In: Príspevok k meteorológii Karpát. Vydavateľstvo Slovenskej akadémie vied v Bratislave, 212–220.

Cheng, L.–AghaKouchak, A., 2015, Nonstationary Rainfall Intensity-Duration-Frequency Curves for Infrastructure Design in a Changing Climate. Scientific Reports Nature. Vol. 4. ISSN 2045-2322. https://doi:org/10.1038/srep07093.

Cheng, L.–Aghakouchak, A.–Gilleland, E.–Katz, R.W., 2014, Non-stationary extreme value analysis in a changing climate. Climate Change. Vol. 27. 353-69. ISSN 0165-0009.

Coles, S., 2001, An introduction to statistical modeling of extreme values. London: Springer-Verlag. ISBN 978-1-4471-3675-0. https://doi:10.1007/978-1-4471-3675-0.

Council Directive 91/271/EEC of 21 May 1991 concerning urban wastewater treatment (OJ L 135, 30.5.1991, 40–52), https://eur-lex.europa.eu/legal-content/EN/TXT/?uri=celex%3A31991L0271.

Dub, O., 1946, Režim veľkých vôd na malých tokoch. Štátny ústav hydrologický. Bratislava.

Dzubák, M., 1969, Stanovenie zákona rozdelenia maximálnych denných zrážkových úhrnov pomocou globálnych čiar prekročenia. Vodohospodársky časopis SAV. Vol 1.

Gaál, L., 2009, Metódy výpočtu štatistických charakteristík návrhových hodnôt úhrnov zrážok na Slovensku. Ostrava: Key Publishing, ISBN 978-80-7418-047-7.

Haiden, T.–Pistotnik G., 2009, Intensity-dependent parameterization of elevation effects in precipitation analysis Adv. Geosci., 20, 33 – 38.

Hofierka, J.–Parajka, J.–Mitašová, H.–Mitaš., L., 2002, Multivariate interpolation of rainfall using regularized spline with tension. Transactions in GIS. 6(2). 135 – 150, https://doi.org/10.1111/1467-9671.00101.

Koutsoyiannis, D., 2004a, Statistics of extremes and estimation of extreme rainfall: I. Theoretical investigation. Hydrological Sciences Journal. Vol. 49. (4), ISSN 2150-3435. https://doi:10.1623/hysj.49.4.575.54430.

Koutsoyiannis, D., 2004b, Statistics of extremes and estimation of extreme rainfall: II. Empirical investigation of long rainfall records. Hydrological Sciences Journal. Vol. 49 (4), ISSN 2150-3435. https://doi:10.1623/hysj.49.4.591.54424.

Koutsoyiannis, D.–Kozonis, D.–Manetas, A., 1998, A mathematical framework for studying rainfall intensity-duration-frequency relationships. Journal of Hydrology. Vol. 206. 118 – 135. ISSN 1879-2707.

Koutsoyiannis, D.–Iliopoulou, T., 2022, Ombrian curves advanced to stochastic modeling of rainfall intensity. Chapter 9. Rainfall. Elsevier. https://doi.org/10.1016/B978-0-12-822544-8.00003-2

Kupčo, M., 1985, Stanovenie krátkodobých zrážkových úhrnov na Slovensku pomocou globálnych čiar prekročenia. Zborník prác SHMÚ. Zv. 25, 1985. Bratislava: ALFA, 9 – 87.

Kupčo, M.–Nejedlík, P.–Onderka. M., 2021, Problém určovania intenzít krátkodobých dažďov na Slovensku. Meteorologický časopis. Vol. 24. 3 – 10. ISSN 1335-339X.

Lutz, J.–Grinde, L.–Dyrrhal, A.V., 2020, Estimating rainfall design values for the city of Oslo. Norway - Comparison of methods and quantification of uncertainty. Water. Vol. 12, 1735. ISSN 2073-4441. https://doi:10.3390/w12061735.

Mitašová, H.–Mitaš, M., 1993, Interpolation with generalized spline with tension: I. Theory and implementation. Mathematical Geology. Vol. 25. 641 – 655. https://doi.org/10.1007/BF00893171.

Onderka, M.–Pecho, J.–Markovič, L.–Nejedlík, P., 2020a, Are rainfall extremes becoming non-stationary due to global warming? A case-study from Slovakia. Meteorologické zprávy. Vol. 73. 138 – 145. ISSN 0026-1173.

Onderka, M.-Pecho, J., 2021, Sensitivity of selected summertime rainfall characteristics to pre-event atmospheric and near-surface conditions. Atmospheric Research. Vol. 259. s. 105671. ISSN 1873-2895. https://doi:10.1016/j.atmosres.2021.105671.

Onderka, M.–Pecho, J.–Nejedlík, P., 2020b, On how rainfall characteristics affect the sizing of rain barrels in Slovakia. Journal of Hydrology - Regional Studies. Vol. 32. s. 100747. ISSN 2214 – 5818. https://doi:10.1016/j.ejrh.2020.100747.

Onderka, M.–Pecho, J., 2022a, Národný klimatický program Slovenskej republiky. Zväzok 17 – 22. Návrhové hodnoty intenzít na Slovensku – lokálne odhady, s 486, Slovenský hydrometeorologický ústav. ISBN 978-80-99929-40-2.

Onderka, M.–Pecho, J.–Bodinger, L.–Bičárová, S.–Lukasová, V., 2022b, Vzťahy medzi intenzitou. trvaním a frekvenciou krátkodobých dažďov určené pomocou bayesovskej inferencie parametrov GEV rozdelenia. Meteorologické zprávy. Vol. 75(3). 81 – 88. ISSN 0026-1173.

Papalexiou, S.M.–Koutsoyiannis, D., 2013, Battle of extreme value distributions: A global survey on extreme daily rainfall. Water Resources Research. Vol. 49. 187 – 201. ISSN 0043-1397. https://doi:10.1029/2012WR012557.

Ragno, E.–Aghakouchak, A.–Cheng, L.–Sadegh M., 2019, A generalized framework for process-informed nonstationary extreme value analysis. Advances in Water Resources. Vol. 130. 270 – 282. ISSN 1872-9657. https://doi:10.1016/j.advwatres.2019.06.007.

Serinaldi, F.–Kilsby, C., 2014, Rainfall extremes: Toward reconciliation after the battle of distributions. Water Resources Research. Vol. 50(1), 336 – 352. ISSN 1944-7973, https://doi:10.1002/2013WR014211.

STN 75 6101, 2002, Slovak Technical Standard 75 6101: Stokové siete a kanalizačné prípojky (Sewer networks and sewage connections). SUTN, Slovak Institute of Technical Standardization, November 2002, 40 p. Consent for quoting was granted by the Office for Standardization, Metrology and Testing of the Slovak Republic under No. ÚNMS/00427/2020-702/000364/2020.

STN EN 16933-2 (75 6111), 2018, Slovak Technical Standard EN 16933-2 (75 6111): Drains and sewer systems outside buildings - Design - Part 2: hydraulic design. ÚNMS SR, Slovak office of Standards, Metrology and Testing, March 2018, 40 p. Consent for quoting was granted by the Office for Standardization, Metrology and Testing of the Slovak Republic under No. ÚNMS/00427/2020-702/000364/2020.

Šamaj, F.–Valovič, Š., 1973, Intenzity krátkodobých dažďov na Slovensku. Zborník prác Hydrometeorologického ústavu. č. 5. s. 84. Bratislava: Slovenské pedagogické nakladateľstvo.

Sherman, C.W., 1932, Frequency and Intensity of Excessive Rainfalls at Boston-Massachusetts. Transactions, ASCE, 95, 951 – 960.

Ulrich, J.–Fauler, F.S.–Rust, H.W.–Rust, H.W., 2021, Modeling seasonal variations of extreme rainfall on different time scales in Germany. Hydrology and Earth Science Systems. Vol. 25. Issue 12, 6133 – 6149, https://doi:10.5194/hess-25-6133-2021.

Urcikán, P.–Imriška, L., 1986, Stokovanie a čistenie odpadových vôd. Tabuľky na výpočet stôk. Bratislava: ALFA-SNTL.